Inorganic Chemistry

ARTICLE

pubs.acs.org/IC

Disproportionation of *O*-Methylhydroxylamine Catalyzed by Aquapentacyanoferrate(II)

María M. Gutiérrez,[†] José A. Olabe,*[,‡] and Valentín T. Amorebieta*[,†]

[†]Department of Chemistry, Facultad de Ciencias Exactas y Naturales, Universidad Nacional de Mar del Plata, Funes y Roca, Mar del Plata B7602AYL, Argentina

[‡]Department of Inorganic, Analytical and Physical Chemistry and INQUIMAE, CONICET, Facultad de Ciencias Exactas y Naturales, Universidad de Buenos Aires, Pabellón 2, Ciudad Universitaria, C1428EHA, Buenos Aires, Argentina

Supporting Information

ABSTRACT: The aquapentacyanoferrate(II) ion, $[Fe^{II}(CN)_5H_2O]^{3-}$, catalyzes the disproportionation reaction of *O*-methylhydroxylamine, NH_2OCH_3, with stoichiometry $3NH_2OCH_3 \rightarrow NH_3 + N_2 + 3CH_3OH$. Kinetic and spectroscopic evidence support an initial N coordination of NH_2OCH_3 to $[Fe^{II}(CN)_5H_2O]^{3-}$ followed by a homolytic scission leading to radicals $[Fe^{II}(CN)_5{}^{\bullet}NH_2]^{3-}$ (a precursor of Fe(III) centers and bound NH_3) and free methoxyl, $CH_3O^{\bullet}$, thus establishing a radical path leading to *N*-methoxyamino ($^{\bullet}NHOCH_3$) and 1,2-dimethoxyhydrazine, $(NHOCH_3)_2$. The latter species is moderately stable and proposed to be the precursor of N_2 and most of the generated CH_3OH. Intermediate $[Fe^{III}(CN)_5L]^{2-}$ complexes (L = NH_3, H_2O) form dinuclear cyano-bridged mixed-valent species, affording a catalytic substitution of the L ligands promoted by $[Fe^{II}(CN)_5L]^{3-}$. Free or bound NH_2OCH_3 may act as reductants of $[Fe^{III}(CN)_5L]^{2-}$, thus regenerating active sites. At increasing concentrations of NH_2OCH_3 a coordinated diazene species emerges, $[Fe^{II}(CN)_5N_2H_2]^{3-}$, which is consumed by the oxidizing $CH_3O^{\bullet}$, giving N_2 and CH_3OH. Another side reaction forms $[Fe^{II}(CN)_5N(O)CH_3]^{3-}$, an intermediate containing the nitrosomethane ligand, which is further oxidized to the nitroprusside ion, $[Fe^{II}(CN)_5NO]^{2-}$. The latter is a final oxidation product with a significant conversion of the initial $[Fe^{II}(CN)_5H_2O]^{3-}$ complex. The side reaction partially blocks the Fe(II)−aqua active site, though complete inhibition is not achieved because the radical path evolves faster than the formation rates of the $Fe^{II}-NO^{+}$ bonds.

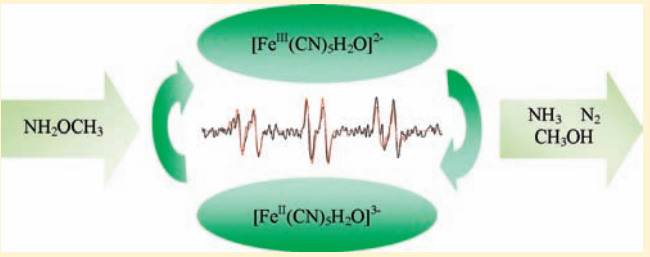

INTRODUCTION

The chemistry and biochemistry of hydroxylamine (NH_2OH) and its substituted alkyl derivatives have been of concern for many years.[1] Recent interest has been developed on the disproportionation reactions of bound NH_2OH and $NH(Me)OH$ and NMe_2OH derivatives[2] as well as on the addition reactions of these nucleophiles to the coordinated nitrosonium ligand.[3] Detailed kinetic and mechanistic studies on disproportionation processes are scarce in the literature.[4] A cursory inspection of available data highlights the crucial significance of coordination of the substrates to metal ions, usually in trace amounts.[5] Also, the high lability of the aqua ions toward substitution (viz., Cu, Fe) makes it difficult to find mechanistic evidence on the coordination step as well as on subsequent chemical events. For the hydroxylamines, a complex picture arises because of the appearance of different oxidation products (variable mixtures of N_2/N_2O and NO_2^-) and intermediates (which may act as inhibitors), and the mechanisms are strongly influenced by the concentration ratio of the substrate/metal ion reactants. By introducing *N*-methyl substituents, significant stoichiometric and mechanistic changes compared with the reactions of NH_2OH have been described.[2]

We used the pentacyano(L)ferrate(II/III) complexes, $[Fe^{II,III}(CN)_5L]^{n-}$, as potential precursors of catalyzed disproportionation.[2] The $[Fe^{II,III}(CN)_5L]^{n-}$ ions are well-characterized systems, forming stable low-spin Fe(II) complexes (typically $K_{st} = 10^3-10^5\ M^{-1}$).[6] They have been studied extensively over the past decades.[7,8] In many cases, the Fe(III) analogs have been also characterized.[6,8] The Fe(II/III) couple might catalyze ligand redox processes on L and could be an interesting reagent in organic oxidation studies.[8]

We extend our studies to the catalyzed disproportionation of *O*-methylhydroxylamine. NH_2OCH_3 is appropriate for preparing *O*-alkyloximes and *O*-alkylhydroxamates,[1b] which are intermediates for production of antibiotics and oxime-type herbicides. It serves as a reagent for the protection and derivatization of keto groups in steroids in order to detect sugars and amino sugars in glycoproteins. It is an active ingredient in several antidiabetes drugs and has been useful in the development of new anticancer therapeutic strategies to overcome tumor resistance. NH_2OCH_3 synergizes with alkylating agents through its reaction with the

Received: April 7, 2011
Published: August 22, 2011

   dx.doi.org/10.1021/ic2007155 | *Inorg. Chem.* 2011, 50, 8817–8825

aldehyde group at the apurinic/apyrimidinic (AP) site on the sugar−phosphate backbones of the cellular DNA. Formation of a DNA−NH_2OCH_3 adduct at the AP site interrupts the base excision repair pathway and is responsible for sustaining DNA damage induced by alkylating agents.[9] In this work, we use detailed mechanistic methodologies, including spin trapping, isotope labeling, and UV−vis/FTIR spectroscopies, in order to disclose the coordination step of NH_2OCH_3 from its subsequent disproportionation reactions as well as for clarifying the different inhibition processes occurring at the active site.

EXPERIMENTAL SECTION

Materials and Methods. *O*-Methylhydroxylamine as the hydrochloride salt $NH_2OCH_3 \cdot HCl$ (methoxyamine hydrochloride), 5,5-dimethyl-1-pyrroline *N*-oxide (DMPO), phenylbutylnitrone (PBN), and 2,2,6,6-tetramethylpiperidine-1-oxyl (TEMPO) were from Aldrich. $NH_2OCH_3 \cdot HCl$ was stored in a desiccator over silica gel. All other chemicals were analytical or reagent grade and used without further purification. Sodium aminopentacyanoferrate(II) trihydrate, $Na_3[Fe^{II}(CN)_5NH_3] \cdot 3H_2O$, was synthesized and purified according to literature procedures.[10] The solid was dried under vacuum over sulfuric acid and stored at 0 °C. ^{15}N-labeled sodium nitroprusside was prepared as described in the literature.[11] Solid K_2HPO_4 was used for preparing 100 mM buffered solutions in deionized water, adding NaCl for reaching an ionic strength of $I = 1$ M. The pH was adjusted to the desired value, 6.1 or 7.1 ± 0.1, by adding a concentrated solution of ∼13 M HCl. Measurements were performed with a Hanna HI 9231 pH meter, supplied with a Hanna HI 1131B glass-body combination electrode, calibrated against Merck standard buffers.

Solutions of NH_2OCH_3 were prepared by dissolving weighed amounts of $NH_2OCH_3 \cdot HCl$ in the argon-bubbled buffered solution and neutralizing the generated HCl with solid NaOH. According to the $pK_a = 4.6$ for the protonated reactant, $NH_3OCH_3^+$,[12] we estimate that NH_2OCH_3 is dominant in our reaction conditions. The $[Fe^{II}(CN)_5H_2O]^{3-}$ ion was generated by dissolving weighed amounts of $Na_3[Fe^{II}(CN)_5NH_3] \cdot 3H_2O$ in the deoxygenated buffer solutions, allowing it to stand for 3−5 min until $[Fe^{II}(CN)_5H_2O]^{3-}$ was totally formed. Solutions were maintained under an argon atmosphere and used within 1 h after preparation to minimize interferences by possible decomposition[13] and eventual conversion of $[Fe^{II}(CN)_5H_2O]^{3-}$ (λ_{max} = 440 nm, ε_{max} = 640 M^{-1} cm^{-1})[14] to $[Fe^{III}(CN)_5H_2O]^{2-}$ (λ_{max} = 394, 340 nm, ε = 750 M^{-1} cm^{-1} for both bands).[15] Mixtures containing dinuclear mixed-valent ions, $[(NC)_5Fe^{III}NCFe^{II}(CN)_4L]^{5-}$ (L = NH_3, H_2O),[16] in equilibrium with mononuclear ions, were obtained from solutions of $[Fe^{II}(CN)_5H_2O]^{3-}$ through O_2 bubbling and used as a control test for the spin-trapping studies as well as for checking their possible activity as catalytic initiators. The concentrations of complex and NH_2OCH_3 were varied in the range 0.05−30 and 0.5−500 mM, respectively. We used the more concentrated solutions for the FTIR/ATR and gas production studies. Independent experiments were performed for studying the reactivity of the $[Fe^{III}(CN)_5H_2O]^{2-}$ or $[Fe^{III}(CN)_5NH_3]^{2-}$ ions (λ_{max} = 400 and 360 nm, ε = 700 and 800 M^{-1} cm^{-1})[17] as oxidants toward NH_2OCH_3. Stock buffer solutions containing $[Fe^{III}(CN)_5NH_3]^{2-}$ were prepared by dissolving weighed amounts of solid $Na_2[Fe^{III}(CN)_5NH_3] \cdot H_2O$, previously synthesized as described in the literature.[18] Solutions showed unchanged spectra during the elapsed time of the studies. Solutions of $[Fe^{III}(CN)_5H_2O]^{2-}$ were obtained from 1 to 2 × 10^{-4} M $[Fe^{III}(CN)_5NH_3]^{2-}$ in the buffer solution by first adjusting the pH to 11. After 15 min, the pH was changed back to pH 6 or 7 with the solution under an argon atmosphere.[19]

UV−vis spectra were acquired with an Ocean Optics HR 2000 CG UV-NIR diode array spectrophotometer in the range 200−1000 nm. A UV−vis−NIR Shimadzu 3101 PC spectrophotometer was used for extending the spectral measurements up to 1400 nm. The fast kinetics was measured with a Hi-Tech Scientific SFA-20 stopped-flow accessory in quartz cuvettes of 1 or 0.2 cm path length. The concentration of the complex was varied between 0.05 and 0.25 mM, with NH_2OCH_3 in enough excess, thus ensuring initial pseudo-order conditions. One of the reservoir syringes of the stopped-flow accessory contained the iron complex and the other NH_2OCH_3. The solutions were directly mixed into the cell, and the data acquisition was started. The values of absorbance against time were processed with standard software.

FTIR/ATR spectra were recorded at room temperature with a Perkin-Elmer Spectrum BX spectrophotometer equipped with a horizontal flat sampling plate accessory of ZnSe, spanning the range 850−1550 and 1750−3100 cm^{-1}. Solutions of ca. 30 mM $[Fe^{II}(CN)_5H_2O]^{3-}$ and ca. 100 mM NH_2OCH_3 were prepared in a dark flask and transferred to the ATR plate with a syringe. The scans were carried out against buffer solutions used as background.

Gas production was quantitatively measured in a thermostated well-stirred closed reactor (0.082 dm^3) linked to an Extrel Emba II mass spectrometer operated at 70 eV and provided with an MKS model 622 absolute transducer for recording the time evolution of the pressure (see Figure SI 1, Supporting Information).[2a] In the experiments, 0.035 dm^3 of a deoxygenated buffered solution of $[Fe^{II}(CN)_5H_2O]^{3-}$, at the desired concentration (0.10−1.5 mM), was placed in the reactor. After evacuation, 0.010 dm^3 of a deoxygenated buffered solution of 10−100 mM NH_2OCH_3 was added and the total pressure was continuously monitored. The mass spectra of the gases in the reactor headspace were acquired at the end of the reaction. The exhausted solutions were examined, searching for other reaction products, CH_3OH, CH_2O, CH_3NH_2, and NH_3, by using specific tests. CH_2O was measured colorimetrically with chromotropic acid.[20] This method was also used to quantify CH_3OH, which was previously oxidized to CH_2O with potassium permanganate in diluted phosphoric acid. NH_3 was determined with the indophenol-blue test[21] and CH_3NH_2 by its reaction with lactulose (4-*O*-β-D-galactopyranosyl-D-fructose) in 1% NaOH.[22] For this test the reaction was carried out in unbuffered mixtures using 50−500 mM NH_2OCH_3. The $[Fe^{II}(CN)_5NO]^{2-}$ ion was identified by FTIR and quantitatively assayed colorimetrically with mercaptosuccinic acid in CO_3^{2-} medium.[23,24]

EPR spectra were acquired at room temperature with a Bruker ER 200D X-band spectrometer operated at ca. 9.79 GHz with a 100 kHz modulation frequency and 1.25 mT of modulation amplitude. The central field and the correct operating frequency were calibrated with regard to a 4 μM aqueous solution of TEMPO as external standard (a_N(NO) = 1.72 mT − g = 2.0051).[25] Free radicals could not be directly detected in the mixed solutions. We used the spin-trapping technique[26,27] with solutions containing ∼50 mM DMPO or ∼0.1 mM PBN, 1.3 mM $[Fe^{II}(CN)_5H_2O]^{3-}$, and 40 mM NH_2OCH_3. The solutions were prepared in a dark flask and transferred into a 0.3 cm^3 EPR quartz flat cell by suction. The first scan was initiated 2−3 min after mixing the solutions. Control experiments were carried out by adding the spin trap to buffered solutions containing representative species of the system: $[Fe^{II}(CN)_5H_2O]^{3-}$, $[(NC)_5Fe^{III}NCFe^{II}(CN)_4H_2O]^{5-}$, NH_2OCH_3, and CH_3OH (Figure SI 2, Supporting Information). Hyperfine coupling constants were determined from spectral simulations using software available from the public site of NIEHS.[28] Numerical simulations of N_2 production were performed using a specific program based on an adaptation of the "predictor-corrector" approach developed by Gear.[29]

RESULTS

The reported chemical transformations of NH_2OCH_3 only occur with previous addition of $[Fe^{II}(CN)_5NH_3]^{3-}$, a precursor of the $[Fe^{II}(CN)_5H_2O]^{3-}$ ion, which contains a labile aqua site.[6,14] No reactivity has been observed either with $[Fe^{II}(CN)_6]^{4-}$ or with

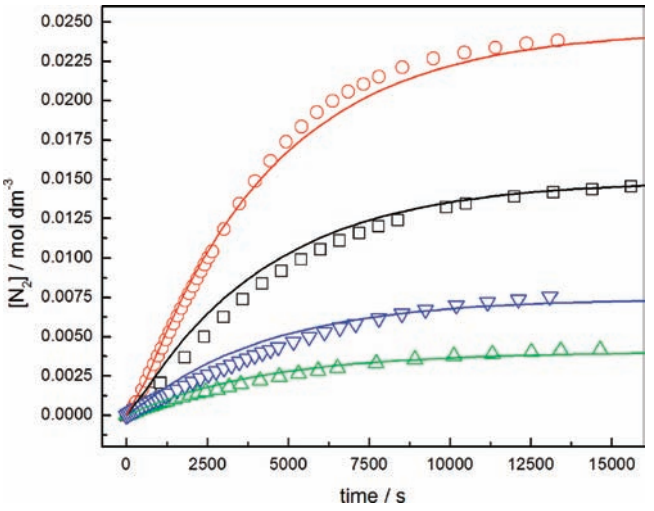

Figure 1. Evolution of the concentration of N_2 against time during the reaction of 1.1 mM $[Fe^{II}(CN)_5H_2O]^{3-}$ with decreasing amounts of NH_2OCH_3: red (circle) 73.8 mM ($R_0 \approx 67$), black (square) 44.9 mM ($R_0 \approx 41$), blue (triangle down) 22.4 mM ($R_0 \approx 20$), and green (triangle up) 12.2 mM ($R_0 \approx 11$), pH 6.2, 25 °C. Lines: concentrations calculated by numerical integration of eqs 2−8c (see Discussion).

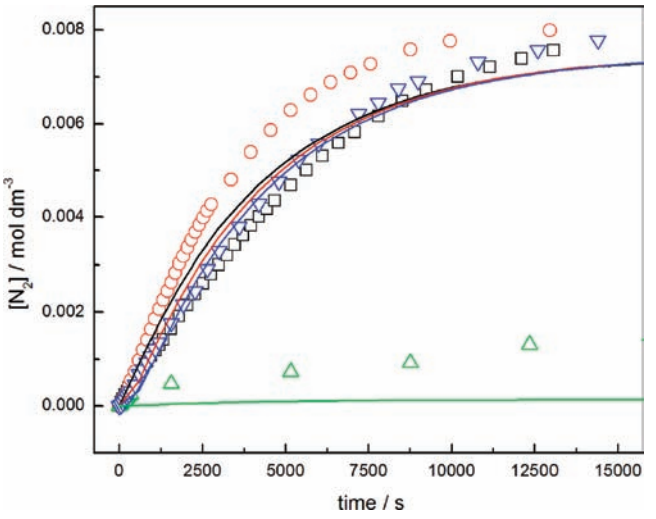

Figure 2. Evolution of the concentration of N_2 against time during the reaction of 22.5 mM NH_2OCH_3 with decreasing amounts of $[Fe^{II}(CN)_5H_2O]^{3-}$: black (square) 1.1 mM ($R_0 \approx 21$), red (circle) 0.29 mM ($R_0 \approx 78$), blue (triangle down) 0.20 mM ($R_0 \approx 113$), and green (triangle up) 0.14 mM ($R_0 \approx 161$), pH 6.2, 25 °C. Lines: concentrations calculated by numerical integration of eqs 2−8c (see Discussion).

the alternative addition of other $[Fe^{II}(CN)_5L]^{3-}$ complexes with Fe^{II}−L bonds inert toward substitution (L = py, substituted pyridines or pyrazines, *S*-bound dimethylsulfoxide, etc.).[30] Pure $[Fe^{III}(CN)_5H_2O]^{2-}$ and $[Fe^{III}(CN)_5NH_3]^{2-}$ ions did not promote disproportionation, in agreement with the fact that the $[Fe^{III}(CN)_5L]^{2-}$ complexes are quite inert toward L substitution (ca. 10^{-7} s^{-1}).[31,32] We introduce the relation $R_0 = [NH_2OCH_3]_0/[Fe^{II}(CN)_5H_2O^{3-}]_0$, the quotient of the initial concentrations of the reactants, which we use in the text.

Stoichiometry of Disproportionation: N_2 Production and Rate Profiles. In the gas production studies with an excess of NH_2OCH_3 at $R_0 > 10$, the mass spectra show that N_2 is the main reaction product with small amounts of CH_4 (1−3% in mass relative to initial $[Fe^{II}(CN)_5H_2O]^{3-}$). Figures 1 and 2 show typical profiles of the concentration of N_2, calculated as if all the produced N_2 is retained in the aqueous phase, against time. The concentration and gas pressure (p_g) are related by $[N_2, \text{mol dm}^{-3}] \approx p_g \times V_g/(RTV_L)$, where V_L and V_g are the volumes of the condensed and gas phases, respectively (see Supporting Information for more details). The traces show clearly the onset of a catalytic reaction given that a small amount of $[Fe^{II}(CN)_5H_2O]^{3-}$ processes large amounts of NH_2OCH_3. N_2 production is independent of pH (range 6−7). From the N_2-production traces, first-order rate constants have been calculated from $[N_2] = [N_2]_\infty \times [1 - \exp(-k_{N2}t)]$, where $[N_2]$ and $[N_2]_\infty$ are the concentrations at time t and ∞, respectively, and $k_{N2} = 1.8 \pm 0.4 \times 10^{-4}$ s^{-1} (Table 1). As we estimated that the rate of transport of N_2 to the gas phase is not limited by the rate of mass transfer through the interface, the measured rate constant may be attributed to a chemical reaction (see Supporting Information).

We identified and quantified CH_3OH, NH_3, and $[Fe^{II}(CN)_5NO]^{2-}$ as other reaction products in the exhausted solutions. Small amounts of CH_2O and CH_3NH_2 are also produced, less than 5% of added NH_2OCH_3. From the concentrations of N_2, NH_3, and CH_3OH (Table 1), the mass balance is within ±10% with regard to the added NH_2OCH_3, thus supporting the stoichiometry described by reaction 1 as the main ongoing catalytic process.

$$3NH_2OCH_3 \rightarrow NH_3 + N_2 + 3CH_3OH \quad (1)$$

By adding more NH_2OCH_3 to the exhausted solutions, production of N_2 proceeds again. In contrast with the exponential increase observed during the first addition, an S-shaped concentration−time profile appears with lower rates of N_2 production. We conclude that enough concentration of active sites for restarting the reaction still remains after the first consumption of NH_2OCH_3. A small fraction of active sites could also be generated through the very slow addition reaction of NH_2OCH_3 to $[Fe^{II}(CN)_5NO]^{2-}$, giving N_2O. However, no N_2O was found, probably because of the poor sensitivity of the mass-spectrochemical technique, cf. ref 33.

Figure 2 shows the results of a set of experiments at constant 22.5 mM NH_2OCH_3 and varying concentrations of iron complex. For the highest $R_0 = 161$, the N_2-production profile differs significantly from the observed one at lower R_0s. At the beginning of the reaction N_2 is produced as before and then decreases noticeably. The spectroscopic studies suggest that the change in the rate is due to the increasing production of $[Fe^{II}(CN)_5N_2H_2]^{3-}$, which acts as an inhibitor, and the reaction rate turns very slow. Production of N_2 may be originated by the oxidative decomposition of $[Fe^{II}(CN)_5N_2H_2]^{3-}$ for low to moderate values of R_0 (see below). At high values, the very slow decay of $[Fe^{II}(CN)_5N_2H_2]^{3-}$ could probably be associated with dissociation and disproportionation or even to oxygen leakage favoring diazene oxidation.

FTIR, EPR, and UV−Vis Spectroscopies. Figure 3 shows the time-dependent FTIR-ATR spectra at pH 6.2 in buffered aqueous solution. The initial stretching band of $[Fe^{II}(CN)_5H_2O]^{3-}$ (ν_{CN}, 2035 cm^{-1}) shifts slightly to 2040 cm^{-1}, and new bands appear at 2090 and 2120 cm^{-1}. These two bands may correspond to ν_{CN} stretchings in $[Fe^{II}(CN)_5L]^{2-}$ and $[(NC)_5Fe^{III}NCFe^{II}(CN)_4L]^{5-}$ complexes containing different L, such as NH_3, H_2O, or other reactive bound intermediates.[7] The bands at

dx.doi.org/10.1021/ic2007155 |*Inorg. Chem.* 2011, 50, 8817–8825

Table 1. Selected Experiments Showing the Concentration of Reactants, Products, and Rate Constants of N_2 Production for the Reaction Between $[Fe^{II}(CN)_5H_2O]^{3-}$ and NH_2OCH_3 (I = 1 M (NaCl), 25 °C)

	$[Fe^{II}(CN)_5H_2O]^{3-}$ mM	NH_2OCH_3 mM	R_0	pH	N_2 mM	NH_3 mM	CH_3OH mM	$10^4 \times k_{N2}$ s^{-1}
1	1.1	73.8	67	6.1	24.0	19.0	67.5	2.1
2	1.1	44.9	41	6.1	14.4	15.2	47.0	1.9
3	1.1	22.4	20	6.1	7.3	6.4	19.0	1.8
4	1.1	12.2	11	6.1	4.2	4.1	13.0	1.6
5	0.29	22.5	76	6.1	8.1	5.4	20.0	1.5
6	0.20	22.5	113	6.1	7.9	6.3	21.0	2.0
7	0.39	43.3	110	7.1	14.4	12.9	40.0	1.9
8	0.39	73.8	189	7.1	25.2	23	72.3	1.8

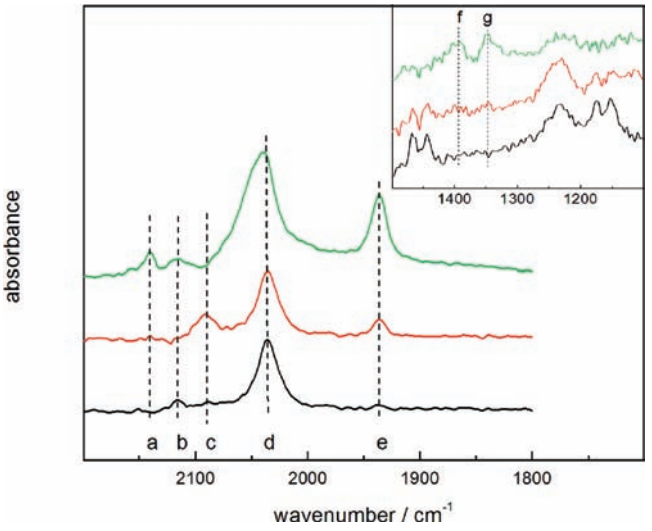

Figure 3. ATR spectra at increasing reaction times (bottom to top) for 0.03 M $[Fe^{II}(CN)_5H_2O]^{3-}$, R_0 = 4, at pH 6.2 and room temperature: 2140 (line a), 2120 (line b), 2090 (line c), 2035−2040 (line d), and 1935 cm^{-1} (line e). (Inset) Spectral changes in the low-energy region: 1390 (line f) and 1354 cm^{-1} (line g).

Table 2. Spin Adducts, Splitting Constants, and g Values

	splitting constants in mT			
detected spin adduct	a_N(NO)	$a_H(H^{\beta})$	$a_H(H^{\gamma})$	g
HDMPO*·OH	1.48	0.10 (2H)		2.0053
DMPO*·OCH_3	1.47	1.07	0.13	2.0053
PBN*·OCH_3	1.51	0.34		2.0053
PBN*·CH_3	1.65	0.35		2.0053

1935 and 2140 cm^{-1} may be confidently assigned to the ν_{NO} and ν_{CN} stretchings in $[Fe^{II}(CN)_5NO]^{2-}$, respectively.[34] Other bands at 1390 and 1354 cm^{-1} have been also found, assignable to a nitroso derivative, see below.

The EPR results are displayed in Table 2.Figure 4 shows a moderately intense spectrum resulting from the contribution of DMPO*·OCH_3 (88% to the total spectrum)[35,36] and HDMPO*·OH spin adducts after mixing $[Fe^{II}(CN)_5H_2O]^{3-}$, DMPO, and NH_2OCH_3. The HDMPO*·OH adduct forms upon hydrolysis and oxidation of DMPO in aqueous solutions, catalyzed by Fe(III) complexes.[37] By using a TEMPO solution as external standard we estimate a maximum concentration of 1−2 μM for the DMPO*·OCH_3 adduct.

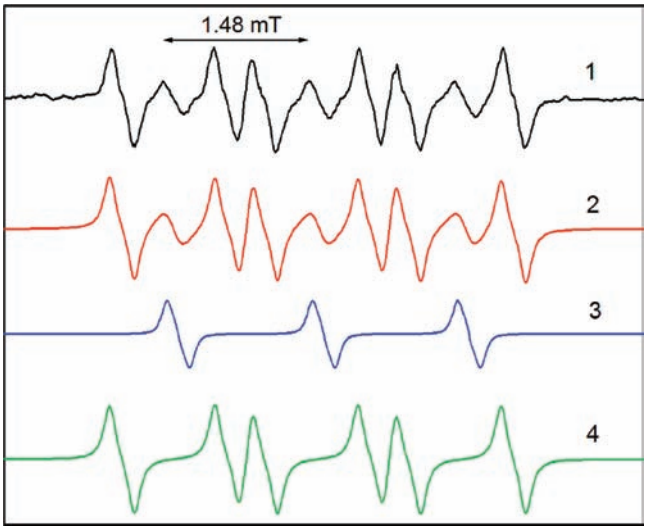

Figure 4. EPR spectra for the reaction of 1.2 mM $[Fe^{II}(CN)_5H_2O]^{3-}$ with 41 mM NH_2OCH_3 ($R_0 \approx 31$) containing 50 mM DMPO in argon-bubbled buffer, pH 6.3, without NaCl. Black (1), experimental spectrum acquired 10 min after DMPO addition; red (2), computer simulation of a mixture of HDMPO*·OH (12% of relative area) and DMPO*·OCH_3 (88% of relative area); blue (3) and green (4), computer simulations of pure HDMPO*·OH and DMPO*·OCH_3, respectively.

By mixing 1.2 mM $[Fe^{II}(CN)_5H_2O]^{3-}$, 0.5 mM PBN, and 40 mM NH_2OCH_3 ($R_0 \approx 33$), well-resolved low-intensity spectra have been obtained (Figure SI 3, Supporting Information). The signals are not very stable and change fast with increasing reaction time. However, the first spectrum exhibits the ^{14}N coupling and the hyperfine structure characteristic of the PBN*·OCH_3 adduct.[38] The latter signal transforms rapidly to the one for the more stable PBN*·CH_3 adduct.[38] We consider that PBN*·CH_3 could be formed by secondary reactions of the PBN*·OCH_3 adduct. We observe a similar evolution by mixing solutions of $[Fe^{II}(CN)_5H_2O]^{3-}$ with NH_2OCH_3 and DMPO (or PBN).

Figures 5 and SI 5, Supporting Information, show the successive UV−vis spectra after mixing solutions of $[Fe^{II}(CN)_5H_2O]^{3-}$ and NH_2OCH_3, R_0 = 10 and 100 respectively. The initial characteristic absorption of $[Fe^{II}(CN)_5H_2O]^{3-}$ at 440 nm[14] decays in a few seconds with subsequent generation of new bands at ca. 362 and 395 nm and a broad absorption in the NIR region (800−1000 nm), which corresponds to a band centered at 1400 nm, typical of members of the mixed-valent series of complexes $[(NC)_5Fe^{III}NCFe^{II}(CN)_4L]^{5-}$ [16] (Figure SI 6, Supporting

dx.doi.org/10.1021/ic2007155 |Inorg. Chem. 2011, 50, 8817–8825

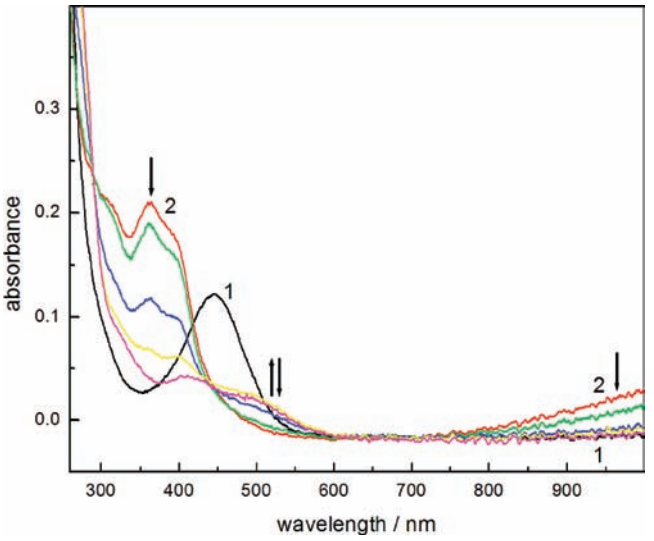

Figure 5. Long-time spectral evolution under typical reaction conditions: 0.2 mM $[Fe^{II}(CN)_5H_2O]^{3-}$ and 2.0 mM NH_2OCH_3 ($R_0 \approx 10$), pH 6.2, 1 M NaCl, 25 °C. Reaction time (in s): black (1), 0; red (2), 90; green, 180; blue, 1200; yellow, 3600; magenta, 10 800.

Information). These last three bands decay subsequently, leading to new transient absorptions at 420 and 480 nm.

For low-to-moderate R_0, namely, <15, the traces for the decay at 440 nm (Figures SI 4a and 4c, Supporting Information) and the nearly simultaneous increase at 362, 395, and 1000 nm can be fitted by a two-exponential model yielding two rate constants, generically k_1 and k_2, in s^{-1}. At 440 nm, the faster decay shows a first-order dependence on $[NH_2OCH_3]$, yielding $k_{fast} = 250 \pm 10\ M^{-1}\ s^{-1}$. The ensuing decay corresponds to $k_{slow} = 0.063\ s^{-1}$, independent of the concentration of NH_2OCH_3. For the absorptions at 362, 395, and 1000 nm, the initial increase of the traces leads to $k'_{fast} = 0.061\ s^{-1}$, i.e., the same value as calculated for k_{slow}. Finally, these bands decrease with $k'_{slow} \leq 10^{-3}\ s^{-1}$.

For $R_0 > 15$ the traces at 440 nm (insets in Figures SI 4b and SI 4c, Supporting Information) display a more complex dependence on time and concentration of NH_2OCH_3 and cannot be fitted by a two-exponential model. After the fast initial decay of the absorptions at 440 nm, new absorptions close to this wavelength appear, depending on R_0, in the time scale of 20−50 s. Figures SI 4b and SI 5, Supporting Information, show that the development and decay of the 360, 390, and 1000 nm bands are nearly simultaneous with the growth of new absorptions between 400 and 500 nm. A limiting situation shows up in Figure SI 7, Supporting Information ($R_0 > 200$). The absorbance of the initial band at 440 nm is followed by the gradual build up of a new, much more intense band at nearly the same wavelength with $\varepsilon > 4000\ M^{-1}\ cm^{-1}$. These absorption properties have been attributed to $[Fe^{II}(CN)_5N_2H_2]^{3-}$, formed in the course of NH_2OH disproportionation.[2a] By maintaining a rigorous anaerobicity, the intense absorption remains unchanged for several days. Under these extreme conditions, no bands in the NIR region assignable to mixed-valent species have been detected[16] and no adducts of DMPO or PBN appear.

DISCUSSION

Disproportionation of NH_2OCH_3. We anticipate a simplified Scheme 1 for describing the reactions involved in the main

Scheme 1

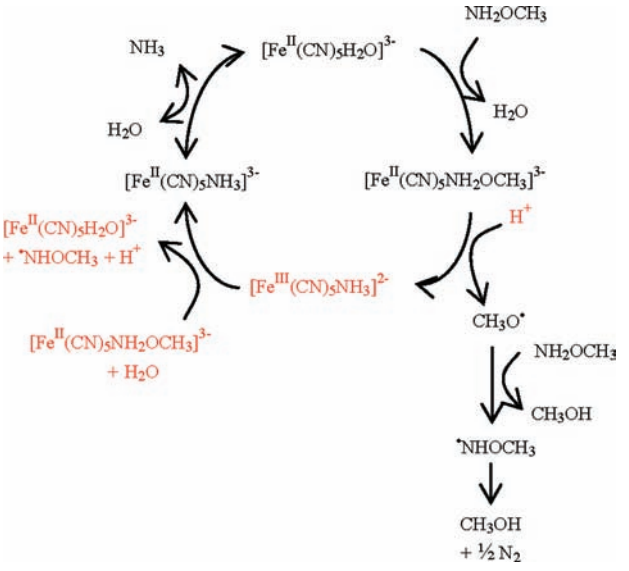

catalytic disproportionation process, eq 1. Upon dissolution of $Na_3[Fe^{II}(CN)_5NH_3]\cdot.3H_2O$, production of $[Fe^{II}(CN)_5H_2O]^{3-}$ occurs in a few minutes ($k_2 = 1.75 \times 10^{-2}\ s^{-1}$),[14] eq 2. At pH 6−7, formation of NH_4^+ allows for full aquation of the amino complex.

$$[Fe^{II}(CN)_5NH_3]^{3-} + H_2O + H^+ \rightarrow [Fe^{II}(CN)_5H_2O]^{3-} + NH_4^+ \quad (2)$$

Reaction 2 sets the scene for coordination of NH_2OCH_3, eq 3.

$$[Fe^{II}(CN)_5H_2O]^{3-} + NH_2OCH_3 \rightleftarrows [Fe^{II}(CN)_5NH_2OCH_3]^{3-} + H_2O \quad k_3, k_{-3} \quad (3)$$

We assign the value of $k_{fast} = 250 \pm 10\ M^{-1}\ s^{-1}$ to k_3 in eq 3, corresponding to decay of the 440 nm band of $[Fe^{II}(CN)_5H_2O]^{3-}$. Similar values have been observed for the coordination rates of a large variety of neutral ligands (NH_3, py, etc.) on $[Fe^{II}(CN)_5H_2O]^{3-}$ at $I = 1$ M, in agreement with a dissociative mechanism, controlled by the release of water.[6,30] We estimate that $k_{-3} \approx 10^{-2}-10^{-4}\ s^{-1}$ by comparing with the L dissociation rates from $[Fe^{II}(CN)_5L]^{3-}$ (L = NH_3, N_2H_4, etc.).[7b]

The $[Fe^{II}(CN)_5NH_2OCH_3]^{3-}$ ion decomposes with homolytic scission of the N−O bond, eq 4, leading to formation of bound $^{\bullet}NH_2$ and free methoxyl radicals, as observed in the spin-trapping studies.

$$[Fe^{II}(CN)_5NH_2OCH_3]^{3-} \rightarrow [Fe^{II}(CN)_5{}^{\bullet}NH_2]^{3-} + CH_3O^{\bullet} \quad k_4 \quad (4)$$

We assign k_{slow}, as well as k'_{fast}, to reaction 4. The $[Fe^{II}(CN)_5{}^{\bullet}NH_2]^{3-}$ ion should transform very rapidly into $[Fe^{III}(CN)_5NH_3]^{2-}$, eq 5, probably through the intermediacy of a ferric amide, Fe(III)−NH_2.[39a] The $[Fe^{III}(CN)_5NH_3]^{2-}$ complex shows a distinctive band at 360 nm,[17] and this is what we observed.

$$[Fe^{II}(CN)_5{}^{\bullet}NH_2]^{3-} + H^+ \rightarrow [Fe^{III}(CN)_5NH_3]^{2-} \quad (5)$$

To simplify, we show in Scheme 1 reactions 4 and 5 as a single step. The intermediacy of $^{\bullet}NH_2/^{\bullet}NH_3^+$ radicals in the reduction of

dx.doi.org/10.1021/ic2007155 |Inorg. Chem. 2011, 50, 8817–8825

NH_2OH to NH_3 by several reductants has been recognized.[1a] Formation of $Cr^{III}NH_3^{3+}$ in the reaction of aqueous Cr(II) with hydroxylamine-*O*-sulfonic acid[40] provides additional support on the coordination of NH_2OCH_3 to Fe(II) through the N atom in eq 3, with subsequent oxidation to Fe(III), eq 5. We found no evidence on the direct oxidation of $[Fe^{II}(CN)_5H_2O]^{3-}$ by $CH_3O^{\bullet}$.

In the second time scale of reactions 4 and 5, the absorption increase at 1000 nm shows that the $[Fe^{III}(CN)_5NH_3]^{2-}$ ion equilibrates with a cyano-bridged mixed-valent complex, eq 6.[16] We estimate values for k_6 and k_{-6} as 10 M^{-1} s^{-1} and 10^{-3} s^{-1}, respectively).[31]

$$[Fe^{III}(CN)_5NH_3]^{2-} + [Fe^{II}(CN)_5H_2O]^{3-} \rightleftarrows [(NC)_5Fe^{III}NCFe^{II}(CN)_4NH_3]^{5-} + H_2O \quad k_6, k_{-6} \qquad (6)$$

We propose that Fe(III) goes back to Fe(II) by reductive cleavage of the mixed-valent complex, eq 7a, or by an outer-sphere redox reaction with $[Fe^{II}(CN)_5NH_2OCH_3]^{3-}$, eq 7b. Both reactions lead to labilization of NH_3 and build up of the *N*-methoxyamino radical, $^{\bullet}NHOCH_3$. The forward rate constant for reaction 7a can be estimated through the observed decay of the intervalence band, leading to $k_{7a} \approx 0.5$ M^{-1} s^{-1}. We estimate $k_{7b} = 10^3$ M^{-1} s^{-1} by an adequate comparison.[41] In reaction 7b, the initial fast electron-interchange between the reactants[41] is irreversibly driven through oxidation of bound NH_2OCH_3 by Fe(III).

$$[(NC)_5Fe^{III}NCFe^{II}(CN)_4NH_3]^{5-} + NH_2OCH_3 + H_2O \rightarrow 2[Fe^{II}(CN)_5H_2O]^{3-} + NH_4^{+} + {}^{\bullet}NHOCH_3 \quad k_{7a} \qquad (7a)$$

$$[Fe^{III}(CN)_5NH_3]^{2-} + [Fe^{II}(CN)_5NH_2OCH_3]^{3-} + 2H_2O \rightarrow 2[Fe^{II}(CN)_5H_2O]^{3-} + NH_4^{+} + {}^{\bullet}NHOCH_3 \quad k_{7b} \qquad (7b)$$

The main reactions associated with the $CH_3O^{\bullet}$ and $^{\bullet}NHOCH_3$ radicals are described in eqs 8a−8c

$$NH_2OCH_3 + CH_3O^{\bullet} \rightarrow CH_3OH + {}^{\bullet}NHOCH_3 \qquad (8a)$$

$${}^{\bullet}NHOCH_3 + {}^{\bullet}NHOCH_3 \rightarrow (NHOCH_3)_2 \qquad (8b)$$

$$(NHOCH_3)_2 \rightarrow N_2 + 2CH_3OH \qquad (8c)$$

On the grounds of its known reactivity, we propose that $CH_3O^{\bullet}$ reacts through a very fast H abstraction with available NH_2OCH_3, eq 8a.[39a,42] Though we have no direct evidence for $^{\bullet}NHOCH_3$, there is a precedent for it being formed as the oxidation product of NH_2OCH_3 with *tert*-butoxy radicals in degassed C_6H_6.[43] $^{\bullet}NHOCH_3$ is not sterically protected at the reactive center and yields 1,2-dimethoxyhydrazine $(NHOCH_3)_2$ through a fast dimerization, eq 8b.[43] This process may be followed by 1,2- or 1,3-hydrogen-atom transfer or by a multistep intermolecular process to give N_2 and CH_3OH, eq 8c.[44,45] It has been possible to oxidize the 1,2-dimethoxyhydrazine intermediate to the corresponding hyponitrite before it decomposes to CH_3OH and N_2.[46] In our interpretation, we propose that 1,2-dimethoxyhydrazine should be sufficiently persistent in the underlying conditions, and its decomposition would determinate the rate of production of N_2, eq 8c. Consequently, the exponential increase of $[N_2]$ production (Figures 1 and 2) can be described by the reaction 1,2-dimethoxyhydrazine → N_2.[47] Equations 2−8c were used for simulation of the profiles of N_2 production using the rate constants detailed in the text. Only k_{8c} was treated as a fitting parameter. The resulting value of 2.4×10^{-4} s^{-1} was used for calculating all the lines displayed in Figures 1 and 2. The one-way sensitivity analysis shows that the shape of the profiles depends strongly on k_{8c} and, to a lesser extent, k_2. The pH-independent rate of the N_2 formation reaction is consistent with this proposal, as no net proton interchange with the medium is operative in step 8c. During the 1-electron oxidation of NH_2OCH_3 by Mn(III) in strongly acid solution,[1m] intermediate $^{\bullet}NHOCH_3$ and a stable 1,2-dimethoxyhydrazine product have been proposed with no release of N_2, however. In contrast, the faster reaction of NH_2OH with Mn(III) leads to N_2 for low values of *R* and to a full oxidation to nitrate for high *R* values.[48]

Secondary Reactions at the Iron(II) Center. The main catalytic process has been discussed in terms of the comparatively fast reactions 2−6 determining initial radical formation, followed by a process with production of NH_3 and regeneration of the catalytic site, $[Fe^{II}(CN)_5H_2O]^{3-}$, eqs 7a and 7b. Reactions 8a−8c complete the stoichiometric picture described by eq 1. We must consider some specific features of the UV−vis spectral evolution (Figures 5 and SI 4 and 5, Supporting Information), indicative of side reaction intermediates, which notoriously do not affect the overall catalytic stoichiometry. We emphasize that the mass balances established formation of N_2, NH_3, and CH_3OH as the products for different values of R_0 (eq 1 and Table 1), irrespective of the nature of the intermediates involved in the reaction.

The transient absorptions at ca. 420−440 for moderate to high values of R_0 (Figures 5 and SI 4−6, Supporting Information) are presently assigned to intermediate formation of a $[Fe^{II}(CN)_5N_2H_2]^{3-}$ complex according to eq 9.[2a,49]

$$[Fe^{III}(CN)_5NH_3]^{2-} + {}^{\bullet}NHOCH_3 \rightarrow [Fe^{II}(CN)_5N_2H_2]^{3-} + CH_3OH + H^{+} \qquad (9)$$

The $[Fe^{II}(CN)_5N_2H_2]^{3-}$ ion is moderately inert toward dissociation of N_2H_2, according to its $\sigma-\pi$ bond properties,[2a,50] though it may be consumed by oxidation through reaction 10.

$$[Fe^{II}(CN)_5N_2H_2]^{3-} + 2CH_3O^{\bullet} + H_2O \rightarrow [Fe^{II}(CN)_5H_2O]^{3-} + N_2 + 2CH_3OH \qquad (10)$$

At increasing concentrations of NH_2OCH_3, reactions 3, 4, and 8a should be favored over the reductive, eqs 7a, 7b, and oxidative processes, eq 10. Reactions 4 and 8a may contribute to production of species leading to $[Fe^{II}(CN)_5N_2H_2]^{3-}$. In Figure SI 7, Supporting Information ($R_0 > 200$), $[Fe^{II}(CN)_5N_2H_2]^{3-}$ traps nearly all the active centers and the reaction evolves much more slowly.

Another band emerges at ca. 480 nm, overlapping with the time period of the 440 nm band. The 480 nm band compares well with the one found at 487 nm under similar conditions for oxidation of *N*-methylhydroxylamine.[2c] It has been traced to an alkylnitroso complex,[2b,51] probably produced by means of initial formation of a *O*-nitrene intermediate followed by the migration of CH_3 to N.[46] By similar comparisons, we assign the weak IR bands in Figure 3, in the 1300−1400 cm^{-1} region, to the $[Fe^{II}(CN)_5N(O)CH_3]^{3-}$ complex.[2b,51−53] Formation of bound

dx.doi.org/10.1021/ic2007155 |*Inorg. Chem.* 2011, 50, 8817–8825

$N(O)CH_3$ implies a two-electron oxidation of $[Fe^{II}(CN)_5NH_2OCH_3]^{3-}$, eq 11. As the band at 480 nm decays further and considering formation of nitroprusside, we propose a subsequent two-electron oxidation, eq 12.

$$[Fe^{II}(CN)_5NH_2OCH_3]^{3-} + 2CH_3O^{\bullet} \rightarrow [Fe^{II}(CN)_5N(O)CH_3]^{3-} + 2CH_3OH \quad (11)$$

$$[Fe^{II}(CN)_5N(O)CH_3]^{3-} + 2CH_3O^{\bullet} + H^+ + H_2O \rightarrow [Fe^{II}(CN)_5NO]^{2-} + 3CH_3OH \quad (12)$$

Reaction 8a is shown to be faster than reaction 11. As a result, $[Fe^{II}(CN)_5NO]^{2-}$ is accumulated toward the end of the reaction, when most of the NH_2OCH_3 has been consumed, without production of N_2O under the catalytic regime, due to the slow addition reaction of NH_2OCH_3 into $[Fe^{II}(CN)_5NO]^{2-}$.[33]

Some comparisons are in order regarding the catalytic disproportionation processes of NH_2OH,[2a] $NH(CH_3)OH$,[2b] and $N(CH_3)_2OH$,[2b] promoted by $[Fe^{II}(CN)_5H_2O]^{3-}$. In all of them, NH_3 and the corresponding NH_2CH_3 and $NH(CH_3)_2$ are produced as the unique 2-electron reduction products. The oxidation products are remarkably different, however, though Fe(II)−Fe(III) cycling has been found with all substrates. Only N_2 is finally produced with NH_2OCH_3, while both N_2 and N_2O are produced with NH_2OH. The N-methylated compounds generate diazomethane, formaldoxime, and other soluble compounds with N(I), though not any gaseous product. The latter situation deals with the strong N−C bonds and lack of a full deprotonation process for allowing gas release. For NH_2OH and NH_2OCH_3, production of radical chains appears as different, depending on the dominant O- or N-coordination mode of the substrate to $[Fe^{II}(CN)_5H_2O]^{3-}$, respectively. For NH_2OH, $^{\bullet}NH_2$ generates a radical chain with production of NH_3 as well as N_2 and N_2O coming from the nitroxyl intermediate, HNO. HNO is the source of nitroprusside, which is attacked by NH_2OH, giving N_2O by an addition route. In contrast, for NH_2OCH_3, N coordination promotes reduction to NH_3 at the iron center and the chain is established with the methoxyl radicals. Remarkably, the time needed for N_2 evolution is around 10-fold lower for NH_2OH than for NH_2OCH_3, for comparable values of *R*, and this is attributed to the different mechanisms for N_2 production. $[Fe^{II}(CN)_5N_2H_2]^{3-}$ has been found as a marginal oxidation intermediate/product for both substrates.

CONCLUSIONS

Disproportionation of NH_2OCH_3 evolves according to the main stoichiometry: $3NH_2OCH_3 \rightarrow NH_3 + N_2 + 3CH_3OH$. Small amounts of the $[Fe^{II}(CN)_5H_2O]^{3-}$ ion process large amounts of NH_2OCH_3 in a catalytic way, initiated by N coordination of the substrate to $[Fe^{II}(CN)_5H_2O]^{3-}$. A key subsequent step is formation of radical species, $^{\bullet}NH_2$ and $CH_3O^{\bullet}$. The $CH_3O^{\bullet}$ radical, characterized by EPR as the spin adduct of DMPO and PBN, is the precursor of $^{\bullet}NHOCH_3$, the *N*-methoxyamino radical, which rapidly dimerizes to the moderately stable 1,2-dimethoxyhydrazine, with ensuing decomposition to N_2 and much of the produced CH_3OH. The bound $^{\bullet}NH_2$ radical is reduced to NH_3, with formation of Fe(III)−NH_3 chromophores, which can be further reduced by free or bound NH_2OCH_3. In this way, $[Fe^{II}(CN)_5H_2O]^{3-}$ can be catalytically regenerated. A side-reaction intermediate has been identified, $[Fe^{II}(CN)_5N_2H_2]^{3-}$, which is produced at increasing values or R_0. At low to moderate R_0 values, bound N_2H_2 is oxidized to N_2, contributing to the main stoichiometry. Inhibition occurs for $R_0 \approx 200$: the very fast production of radicals leads to saturation of the Fe(II) complex with N_2H_2 with suppression of catalysis. Another side reaction comprises the successive 2-electron oxidations of NH_2OCH_3 to nitrosomethane, $N(O)CH_3$, and nitroprusside, $[Fe^{II}(CN)_5NO]^{2-}$. The latter is unreactive toward NH_2OCH_3 in the underlying conditions. We conclude that catalytic disproportionation evolves at a sufficiently greater rate compared to the oxidation reactions, favoring catalysis in spite of a partial blocking of the active site by NO^+.

ASSOCIATED CONTENT

Supporting Information. Diagram of the reactor; EPR spectra in argon-bubbled buffered solutions for the reaction between DMPO and $[(NC)_5Fe^{III}NCFe^{II}(CN)_4H_2O]^{5-}$, $[(NC)_5Fe^{III}NCFe^{II}(CN)_4H_2O]^{5-}$ plus CH_3OH, NH_2OCH_3; computer simulations of the EPR spectra of the spin adducts of $PBN^*\cdot OCH_3$ and $PBN^*\cdot CH_3$; subsequent UV−vis spectra at short times after mixing, with traces at 440 nm; successive spectra for $R_0 \approx 100$; UV−vis−NIR spectrum obtained during reaction of 1.5×10^{-4} M $[Fe^{II}(CN)_5H_2O]^{3-}$ and 1.75×10^{-3} M NH_2OCH_3; long time accumulation of the $[Fe^{II}(CN)_5N_2H_2]^{3-}$ complex for $R_0 = 204$; relationship between pressure and total N_2 concentration in the condensed phase; estimation of the rate of transport of N_2 to the gas phase. This material is available free of charge via the Internet at http://pubs.acs.org.

AUTHOR INFORMATION

Corresponding Author

*E-mail, amorebie@mdp.edu.ar (V.T.A.); olabe@qi.fcen.uba.ar (J.A.O.).

ACKNOWLEDGMENT

We thank the Universities of Buenos Aires and Mar del Plata, the National Scientific Council (CONICET), and the National Funding Agency, ANPCYT, for economic support. V.T.A. and J.A.O. are members of the scientific staff of CONICET.

REFERENCES

(1) (a) Wieghardt, K. *Adv. Inorg. Bioinorg. Mech.* **1984**, *3*, 213. (b) In *The Chemistry of Hydroxylamines, Oximes and Hydroxamic Acids*; Rappoport, Z., Liebman, J. F., Eds.; Wiley: New York, 2008. (c) Gross, P. *Crit. Rev. Toxicol.* **1985**, *14*, 87. (d) Stedman, G. Adv. *Inorg. Chem. Radiochem.* **1979**, *22*, 113. (e) Hung, M. L.; McKee, M. L.; Stanbury, D. M. *Inorg. Chem.* **1994**, *33*, 5108. (f) Makarycheva-Mikhailova, A. V.; Stanbury, D. M.; McKee, M. L. *J. Phys. Chem. B* **2007**, *111*, 6942. (g) Liu, R. M.; McDonald, M. R.; Margerum, D. W. *Inorg. Chem.* **1995**, *34*, 6093. (h) Johnson, M. D.; Hornstein, B. J. *Inorg. Chem.* **2003**, *42*, 6923. (i) Lockamy, V. L.; Shields, H.; Kim-Shapiro, D. B.; King, S. B. *Biochim. Biophys. Acta* **2004**, *1674*, 260. (j) Benjamin, E.; Hijjy, Y. *Molecules* **2008**, *13*, 157. (k) Albertin, G.; Antoniutti, S.; Bravo, J.; Castro, J.; García-Fontan, S.; Martin, M. C.; Noe, M. *Eur. J. Inorg. Chem.* **2006**, 3451. (l) Wu, A.; Mader, E. A.; Datta, A.; Hrovat, D. A.; Borden W. T. Mayer, J. M. *J. Am. Chem. Soc.* **2009**, *131*, 11985. (m) Davies, G.; Kustin, K. *Inorg. Chem.* **1969**, *8*, 484. (n) Honig, D. S.; Kustin, K.; Martin, J. F. *Inorg. Chem.* **1972**, *11*, 1895. (o) Swaroop, R.; Gupta, Y. K. *J. Inorg. Nucl. Chem.* **1974**, *36*, 169.

(2) (a) Alluisetti, G. B.; Almaraz, A. E.; Amorebieta, V. T.; Doctorovich, F.; Olabe, J. A. *J. Am. Chem. Soc.* **2004**, *126*, 13432. (b) Gutiérrez, M. M.; Alluisetti, G. B.; Gaviglio, C.; Doctorovich, F.; Olabe, J. A.; Amorebieta,

V. T. *Dalton Trans.* **2009**, 1187. (c) Bari, S. E.; Amorebieta, V. T.; Gutiérrez, M. M.; Olabe, J. A.; Doctorovich, F. *J. Inorg. Biochem.* **2010**, *104*, 30. (d) Choi, I.; Liu, Y.; Wei, Z.; Ryan, M. D. *Inorg. Chem.* **1997**, *36*, 3113. (e) Bazylinski, D. A.; Arkowitz, R. A.; Hollocher, T. C. *Arch. Biochem. Biophys.* **1987**, *259*, 520.

(3) (a) Gutiérrez, M. M.; Alluisetti, G. B.; Olabe, J. A.; Amorebieta, V. T. *Dalton Trans.* **2008**, 5025. (b) Olabe, J. A.; Estiú, G. L. *Inorg. Chem.* **2003**, *42*, 4873. (c) Wolfe, S. K.; Andrade, C.; Swinehart, J. H. *Inorg. Chem.* **1974**, *13*, 2567.

(4) (a) In *Comprehensive Coordination Chemistry*; Gillard, R. D., McCleverty, J. A., Eds.; Elsevier Ltd.: New York, 1987. (b) In *Comprehensive Coordination Chemistry II*; McCleverty, J. A., Meyer, T. J., Eds.; Elsevier Ltd.: New York, 2004.

(5) (a) Lunak, S.; Veprek-Siska, J. *Collect. Czech. Chem. Commun.* **1974**, *39*, 41. (b) Lunak, S.; Veprek-Siska, J. *Collect. Czech. Chem. Commun.* **1974**, *39*, 391. (c) Bonner, F. T.; Akhtar, M. J. *Inorg. Chem.* **1981**, *20*, 3155. (d) Bridgart, G. J.; Waters, W. A.; Wilson, I. R. *J. Chem. Soc., Dalton Trans.* **1973**, 1582.

(6) (a) Toma, H. E.; Malin, J. M. *Inorg. Chem.* **1973**, *12* (1039), 2080. (b) Toma, H. E.; Malin, J. M. *J. Am. Chem. Soc.* **1975**, *97*, 288.

(7) (a) Olabe, J. A. *Dalton Trans.* **2008**, 3633. (b) Baraldo, L. M.; Forlano, P.; Parise, A. R.; Slep, L. D; Olabe, J. A. *Coord. Chem. Rev.* **2001**, *219*−*221*, 881. (c) Macartney, D. H. *Rev. Inorg. Chem.* **1988**, *6*, 101.

(8) Olabe, J. A. *Adv. Inorg. Chem.* **2004**, *55*, 61.

(9) (a) Liao, Y.; Syn, M.; Xu, Y. *J. Liq. Chromogr. Related Technol.* **2002**, *28*, 2433 and references cited therein. (b) Wang, E.; Struble, E.; Liu, P.; Cheung, A. P. *J. Pharm. Biomed. Anal.* **2002**, *30*, 415 and references cited therein.

(10) Kenney, D. J.; Flynn, T. P.; Gallini, J. B. *J. Inorg. Nucl. Chem.* **1961**, *20*, 75.

(11) Chacón Villalba, M. E.; Varetti, E. L.; Aymonino, P. J. *Vib. Spectrosc.* **1997**, *14*, 275.

(12) Bissot, T. C.; Parry, R. W.; Campbell, D. H. *J. Am. Chem. Soc.* **1957**, *79*, 796.

(13) Olabe, J. A.; Zerga, H. O. *Inorg. Chem.* **1983**, *22*, 4156.

(14) Toma, H. E. *Inorg. Chim. Acta* **1975**, *15*, 205.

(15) Espenson, J. H.; Wolenuk, S. G., Jr. *Inorg. Chem.* **1972**, *11*, 2034.

(16) (a) Emschwiller, G. *C. R. Acad. Sci. Paris* **1967**, *265*, 281. (b) Emschwiller, G.; Jorgensen, C. K. *Chem. Phys. Lett.* **1970**, *5*, 561. (c) Souto, M. F.; Cukiernik, F. D.; Forlano, P.; Olabe, J. A. *J. Coord. Chem.* **2001**, *54*, 343.

(17) Gale, R.; McCaffery, A. J. *J. Chem. Soc., Dalton Trans.* **1973**, 1344.

(18) Brauer, G. *Handbook of Preparative Inorganic Chemistry*, 2nd ed.; Academic Press: New York, 1965.

(19) Macartney, D. H.; Mc Auley, A. *Can. J. Chem.* **1981**, *59*, 132.

(20) *NIOSH Manual of Analytical Methods, Method N° 3500*, 4th ed.; 1994.

(21) Koroleff, F. In *Methods of Seawater Analysis*; Grasshoft, K., Ed.; Verlag Chemie: New York, 1976.

(22) Adachi, S. *Anal. Chem.* **1965**, *37*, 896.

(23) Szacilowski, K.; Stochel, G.; Stasicka, Z.; Kisch, H. *New J. Chem.* **1997**, *21*, 893.

(24) Roncaroli, F.; Olabe, J. A.; van Eldik, R. *Inorg. Chem.* **2002**, *41*, 5417.

(25) Testa, J. J.; Grela, M. A.; Litter, M. I. *Environ. Sci. Technol.* **2004**, *38*, 1589.

(26) Janzen, E. G. *Acc. Chem. Res.* **1971**, *4*, 31.

(27) Rehorek, D. *Chem. Soc. Rev.* **1991**, *20*, 341.

(28) Niehs spin trap database: http://tools.niesh.nih.gov/stdb/index.cfm.

(29) Gear, C. W. *Comun. ACM* **1971**, *14*, 176.

(30) Toma, H. E.; Batista, A. A.; Gray, H. B. *J. Am. Chem. Soc.* **1982**, *104*, 7509.

(31) James, A. D.; Murray, R. S.; Higginson, W. C. E. *J. Chem. Soc., Dalton Trans.* **1974**, 1273.

(32) The solids containing Fe(III)−aqua, prepared according to ref 18, were shown to be active toward catalytic disproportionation. However, we found small (2−3%) impurities of Fe(II) in the relevant freshly prepared solutions, as demonstrated by the reaction with isonicotinamide leading to $[Fe^{II}(CN)_5(\text{isonicotinamide})]^{3-}$ (cf. ref 6). By adding isonicotinamide, catalysis was suppressed, thus revealing that the predominant $[Fe^{III}(CN)_5H_2O]^{2-}$ ion in solution was unreactive. On the other hand, Fe(III)−L inert complexes may undergo L substitution, catalyzed by Fe(II) complexes, in the presence of small amounts of reductants (cf. ref 31). We confirmed in an independent experiment that freshly prepared solutions of the dinuclear, cyano-bridged mixed-valent complex were also active toward disproportionation catalysis.

(33) As nitroprusside might be engaged in further reactions with the species involved in the disproportionation process of NH_2OCH_3, we started the reaction by adding labeled $[Fe^{II}(CN)_5{}^{15}NO]^{2-}$ to the reacting mixture. Mass spectral analysis showed no evidence of labeled gaseous products, so that we may discard its participation in the overall process. NH_2OCH_3 reacts with nitroprusside through a very slow reaction, producing N_2O + CH_3OH, with $t_{1/2}$ = 2.3 h (Amorebieta, V. T. Work in progress).

(34) Schwane, J. D.; Ashby, M. T. *J. Am. Chem. Soc.* **2002**, *124*, 6822.

(35) Guo, Q.; Qian, S. Y.; Mason, R. P. *J. Am. Soc. Mass Spectrom.* **2003**, *14*, 862.

(36) Dikalov, S. I.; Mason, R. P. *Free Radical Biol. Med.* **1999**, *27*, 864.

(37) Makino, K.; Hagi, A.; Ide, H.; Murakami, A. *Can. J. Chem.* **1992**, *70*, 2818.

(38) Britigan, B. E.; Coffman, T. J.; Buettner, G. R. *J. Biol. Chem.* **1990**, *265*, 2650.

(39) (a) Stanbury, D. M. in *Physical Inorganic Chemistry. Reactions, Processes and Applications*; Bakac, A., Ed.; Wiley: New York, 2010; Chapter 9, p 409. (b) Simic, M.; Hayon, E. *J. Am. Chem. Soc.* **1971**, *93*, 5982. (c) Neta, P; Maruthamuthu, P.; Carton, P. M.; Fessenden, R. W. *J. Phys. Chem.* **1978**, *82*, 1875.

(40) Bakac, A.; Simunic, J. L.; Espenson, J. H. *Inorg. Chem.* **1990**, *29*, 1090.

(41) Stasiw, R.; Wilkins, R. G. *Inorg. Chem.* **1969**, *8*, 156.

(42) Kochi, J. K. *Free Radicals*; Wiley: New York, 1973; Vol. II.

(43) A reviewer noted that $CH_3O^{\bullet}$ decomposes in a unimolecular way, giving the CH_2OH radical, with $k \approx 10^5\ s^{-1}$. Thus, the rate constant of reaction 8a should be at least $10^9\ M^{-1}\ s^{-1}$, allowing it to evolve in our reaction conditions, R_0 = 10−100.

(44) Kaba, R. A.; Ingold, K. U. *J. Am. Chem. Soc.* **1976**, *98*, 7375.

(45) Malatesta, B.; Ingold, K. U. *J. Am. Chem. Soc.* **1974**, *96*, 3949.

(46) Carey, F. A.; Hayes, L. J. *J. Org. Chem.* **1973**, *38*, 3107.

(47) The N_2-production curves represent a typical accumulation process affording first-order kinetics. The curves have been adequately fitted, and from the traces we can see that the molar concentrations of N_2 at the end of the reaction are ∼1/3 the initial concentrations of NH_2OCH_3. We thus interpret that N_2 production relates to a scheme $X \rightarrow N_2$. The experiments do not define species X. In the first step of the mechanism, we show that the rate is first order in NH_2OCH_3 and first order in $[Fe^{II}(CN)_5H_2O]^{3-}$. As the reaction is catalytic, except during the very short initial period and when NH_2OCH_3 has been nearly totally consumed, the cycle will operate in steady-state conditions and the concentrations of both species will remain constant. Therefore, the reaction rate should be constant during most of the reaction period. We should not observe a constant rate if the concentration of active sites decayed because stable species were trapping the sites (our results only suggest a partial inhibition). In a crucial experiment (Figure 2, Table 1) we show that for constant $[NH_2OCH_3]$ and changing [Fe] by a factor of 5 we do not observe changes in the rate of N_2 production. We interpret these results by saying that N_2 production is independent of the steady-state concentration of active centers and, consequently, of the initial concentration of $[Fe^{II}(CN)_5H_2O]^{3-}$. We are proposing that the slow N_2 production corresponds with the decomposition of 1,2-dimethoxyhydrazine and not with that from NH_2OCH_3. As a result, the instantaneous concentrations of N_2 do not relate to the instantaneous concentrations of NH_2OCH_3 but, instead, with that from 1,2-dimethoxyhydrazine, i.e., $k_{N2} \approx k_{8c}$.

(48) In refs 1m and 1n, the slower oxidation rates of NH_2OCH_3 compared to NH_2OH by Mn(III) and Ag(II) were traced to different hydrogen-bonding effects. On the other hand, it could be argued that the stronger N−O bond compared to the N−H bond makes N_2 evolution more difficult.

(49) Alternative production of $[Fe^{II}(CN)_5N_2H_2]^{3-}$ could be achieved through fast formation of radicals according to reaction 4, favoring formation of a hydrazine complex by dimerization of $^{\bullet}NH_2$ radicals with subsequent oxidation by the methoxyl radicals.

(50) Lehnert, N.; Wiesler, B. E.; Tuczek, F.; Hennige, A.; Sellmann, D. *J. Am. Chem. Soc.* **1997**, *119*, 8869.

(51) Cheney, R. P.; Simic, M. G.; Hoffman, M. Z.; Taub, I. A.; Asmus, K. D. *Inorg. Chem.* **1977**, *16*, 2187.

(52) Socrates, G. *Infrared Characteristic Group Frequencies. Tables and Charts*, 2nd ed.; Wiley: New York, 1998.

(53) Cheney, R. P.; Pell, S. D.; Hoffman, M. Z. *J. Inorg. Nucl. Chem.* **1979**, *41*, 489.